Earthquakes and Structures, *Vol. 7, No. 1 (2014) 83-99*
DOI: http://dx.doi.org/10.12989/eas.2014.7.1.083

Higher-mode effects for soil-structure systems under different components of near-fault ground motions

Faramarz Khoshnoudian[1a], Ehsan Ahmadi[*1], Sina Sohrabi[2b] and Mahdi Kiani[3c]

[1]*Department of Civil Engineering, Amirkabir University of Technology (Tehran Polytechnic), Hafez Ave., Tehran, Iran*
[2]*School of Engineering, Shiraz University, Zand Ave., Shiraz, Iran*
[3]*Deprtment of Civil Engineering, Babol Noshirvani Institue of Technology, Babol, Iran*

(Received August 27, 2013, Revised March 1, 2014, Accepted March 4, 2014)

Abstract. This study is devoted to estimate higher-mode effects for multi-story structures with considering soil-structure interaction subjected to decomposed parts of near-fault ground motions. The soil beneath the super-structure is simulated based on the Cone model concept. Two-dimensional structural models of 5, 15, and 25-story shear buildings are idealized by using nonlinear stick models. The ratio of base shears for the soil-MDOF structure system to those obtained from the equivalent soil-SDOF structure system is selected as an estimator to quantify the higher-mode effects. The results demonstrate that the trend of higher-mode effects is regular for pulse component and has a descending variation with respect to the pulse period, whereas an erratic pattern is obtained for high-frequency component. Moreover, the effect of pulse component on higher modes is more significant than high-frequency part for very short-period pulses and as the pulse period increases this phenomenon becomes vice-versa. SSI mechanism increases the higher-mode effects for both pulse and high-frequency components and slenderizing the super-structure amplifies such effects. Furthermore, for low story ductility ranges, increasing nonlinearity level leads to intensify the higher-mode effects; however, for high story ductility, such effects mitigates.

Keywords: near-fault ground motions; high-frequency effects; higher-mode effects; soil-structure interaction; multiple story structures

1. Introduction

Ground motions in the proximity of active faults have some prominent features that make them different from far-fault ground motions. Fling step and forward directivity effects are the two prominent properties of near-fault ground motions which can significantly affect the response of structures. The fling step is due to the static displacement arising from fault motions. The forward

*Corresponding author, Graduated M.Sc,, E-mail: ehsanahmadi@aut.ac.ir
[a]Associate Professor, E-mail: khoshnoud@aut.ac.ir
[b]Ph.D. Student, E-mail: sinasohrabi@shirazu.ac.ir
[c]Ph.D. Student, E-mail: mahdikiani@aut.ac.ir

directivity emanates from the fault rupture once occurs at a velocity same as the shear-wave velocity of the site. Between these two important effects, the forward directivity is intended to be discussed in this study. Many studies have been carried out to capture the salient properties of near-fault ground motions with the forward directivity effect (Somerville *et al*. 1997, Spudich and Chiou 2008, Seekings and Boatwright 2010). Somerville (2000) made attempts to shed light on the particular effects of forward directivity. Mavroeidis and Papageorgiou (2002, 2003) investigated characteristics of near-fault ground motions and suggested an expression to mimic the pulse component of near-fault ground motions. Mavroeidis *et al*. (2004) elucidated that such pulses are capable to significantly affect their corresponding spectrum. Hubbard and Mavroeidis (2011) stated that forward directivity pulses can considerably influence the damping modification factors. Tang and Zhang (2011) proposed an approach to recognize the pulses available in near-fault ground motions. Iervolino *et al*. (2012) investigated the inelastic displacement ratios under near-fault ground motions and suggested a formula to calculate inelastic displacement ratios based on the pulse period. As well, near-fault ground motions can significantly affect the response of structures (Mylonakis and Reinhorn 2001, Zhang and Iwan 2002, Kam *et al*. 2010, Mylonakis and Voyagaki 2006). Alavi and Krawinkler (2004) studied the responses of multi-story frame structures under both near-fault and ordinary ground motions and a comparison reveals that near-fault ground motions are capable to enforce higher demands to the studied structures. Kalkan and Kunnath (2006) concluded that higher stories experiences higher demands than lower ones due to the both forward and fling step pulses. Sehhati *et al*. (2011) investigated the story ductility distribution over the structural height under ordinary and near-fault ground motions and inferred that upper stories experience much more demands than lower ones for near-fault ground motions. All the studies, noted previously, have been carried out for structures with fixed-base condition and there were no trace of soil flexibility.

Some researchers put efforts into decomposing near-fault records by different approaches. Baker (2007) employed wavelet analysis to separate pulse and high-frequency parts of near-fault records. The high-frequency part was the result of subtracting the original record from the pulse component and was quoted as the residual record in Baker's study. Xu and Agrawal (2010) adopted the empirical mode decomposition (EMD) to segregate the dominant pulse and high-frequency components of near-fault ground motions. Ghahari *et al*. (2010) utilized a moving average filtering with a suitable frequency cut-off to decompose near-fault records. In their investigation, pulse and high-frequency parts of a record were quoted as the Pulse-Type Record (PTR) and Back-Ground Record (BGR). Besides the pulse component of near-fault ground motions, the high-frequency component of a near-fault record might considerably affect the structural response. Significance of the high-frequency part of such records was also noted by other researchers (Ghobarah 2004, Makris and Roussos 1998, Elsheikh and Ghobarah 2004). Somerville (2000) demonstrated that acceleration response spectra of near-fault records for moderate-to-large earthquakes are stronger than those obtained for very large earthquakes in the high frequency range. Similar results also were observed by Mavroeidis and Papageorgiou (2002, 2003). Mavroeidis *et al*. (2004) verified that the stronger earthquakes exhibit rich contents in low frequency ranges (long-period pulses), whereas the smaller earthquakes are specified by high-frequency components. It should be noted that in the previous studies, the main focus was on the seismology aspect of near-fault records. Ghobarah (2004) investigated engineering aspects of the

high-frequency component and revealed that the high-frequency portion of a near-fault record can be important, particularly for short-period structures. He investigated only near-fault ground motions with long-period pulses and concluded that long-period pulses may affect the fundamental mode of structures and the high-frequency component may comply with the higher modes leading to significant total responses for structures. Elsheikh and Ghobarah (2004) verified that high-frequency content of a near-fault record can influence the demands of stiff structures. However, these studies did not address a definite pattern for the effects of each component (pulse and high-frequency). All the previous studies were done on fixed-base structures and SSI effects have been disregarded.

On the other hand, the Soil–Structure Interaction (SSI) mechanism significantly impresses the dynamic properties of the super-structure. Elastic demands of structures were evaluated by many researchers considering SSI effects (Chopra and Gutierrez 1974, Novak 1974, Veletsos 1977). Nonlinear responses of soil-structure systems were also scrutinized (Bielak 1978, Muller and Keintzel 1982, Rodriguez and Montes 2000, Aviles and Perez-Rocha 2003). Studies showed that ductility and strength demands of structures experience notable changes due to the SSI effects (Ghannad and Ahmadnia 2006). Also, it was demonstrated that hysteretic energy of the structure is significantly affected by the interaction phenomenon (Nakhaei and Ghannad 2004). Aviles and Perez-Rocha (2003, 2005) made attempts to include the SSI effects into the nonlinear behavior of structures through modifying the strength reduction factor. Aviles and Perez-Rocha (2011) proposed a new technique to obtain the displacement demand associated with strain in the super-structure by removing rigid body motions of the foundation from the global displacement of the soil-structure system. It was shown that SSI effects also can change the damage index of buildings (Nakhaei and Ghannad 2008). Although the demands of soil-structure systems were investigated under ordinary ground motions, effects of different portions associated with near-fault ground motions, particularly the pulse and high-frequency have been ignored.

As previously noted, the soil-structure mechanism and different portions of near-fault ground motions can extremely affect structural responses. Also, it is very desirable for structural engineers to compute the seismic responses of actual MDOF structures by substituting them with simplified equivalent SDOF oscillators. In such cases, higher-mode effects show their efficiency which might prevent a structural engineer from using an equivalent SDOF oscillator. In addition, in many studies, researchers ignore the high-frequency part of records and use the distinctive main pulse part of records in their analyses. From this viewpoint, there is a lack of knowledge in the case of high-frequency effects on the higher modes for both fixed-base structures and soil-structure systems. Therefore, the primary goal of this study is to elucidate the impacts of the two decomposed components of near-fault records, i.e., pulse and high-frequency parts, on the higher modes of multi-story structures including soil effects and clarify that what component triggers higher modes with more intensity. Such issue has not been addressed so far not only for fixed-base structures, but also for soil-structure systems. A suite of 64 original near-fault records and their corresponding components extracted by Baker (2007) are adopted. Non-dimensional frequency, aspect ratio, and target story ductility of the super-structure are selected as the main parameters of the soil-structure system. The two-dimensional structural models of 5, 15, and 25-story shear buildings and their corresponding equivalent SDOF oscillators are analyzed and the ratios of their base shears are chosen to detect the severity of higher-mode effects.

2. Soil-structure simulation and governing parameters

In this study, as it is shown in Fig. 1, the super-structure and the soil are modeled based on the stick model and Cone model concept, respectively. When story shear mechanisms are expected (e.g., strong beam/weak column frames), a stick model can be employed. The end of the simplified models is to concise computational and data management efforts. More consequentially, they can also provide a perceivable visualization tool for engineers (FEMA 440). Takewaki (1998) proposed a new ductility design method for soil-structure systems using a shear building model for the superstructure. Furthermore, Shimming and Gang (1998) used a same model in order to simulate frame structures and frame-shear wall structures. However, it should be noted that a stick model can overestimate the higher-mode response that might not present or not so sever as in a corresponding frame model. For example, if the yielding occurs at the base of a stick model, a number of the top stories of the model will have very large accelerations even if all other stories do not yield and the results from a corresponding frame model would have much less accelerations than a stick model. In order to consider the nonlinear behavior of each story, the bilinear behavior with the strain hardening ratio of 5 % is assumed for the overall force-relative displacement of each story. The higher-mode response in the upper stories of the buildings is unlikely to be caused by the use of stick models because a moderate post-yield stiffness of 5% is used for all stories. Two-dimensional structural models of 5, 15, and 25-story shear buildings are studied with respectively fundamental fixed-base periods of 0.7, 1.5, and 2.3 sec. The viscous damping ratio of the super-structure is incorporated into the system on the basis of Rayleigh's damping concept and also, the stiffness is distributed over the height of the super-structure based on the equivalent seismic lateral force given in ASCE07-10. The nonlinearity level in the super-structure is controlled by the maximum story ductility. Maximum story ductility is defined as the peak of ductility among all stories. Values of 2, 4, and 8 are assigned to this parameter. Each property associated with i^{th} story is designated by the subscript of i. m_i, I_i , and r_i respectively symbolize the mass, the mass moment of inertia around its geometric center, and the radius of the equivalent circular plan in the i^{th} story from the foundation surface. The same features are postulated for all stories. The height and effective load (dead as well as live load) for each story are assumed 3.3 m and 10 kN/m^2 as for typical buildings. In order to estimate higher-mode effects, the equivalent SDOF oscillator is constructed based on the recommendation of FEMA 440[36]. It is described by first mode properties of the MDOF super-structure. The equivalent mass, m_e, and equivalent height, H_e, are computed as following:

$$m_e = (\sum_{i=1}^{n} m_i \phi_i)^2 \Big/ \sum_{i=1}^{n} m_i \phi_i^2 \tag{1}$$

$$h_e = \sum_{i=1}^{n} m_i \phi_i h_i \Big/ \sum_{i=1}^{n} m_i \phi_i \tag{2}$$

The vibration period of the equivalent oscillator, T_e, corresponds to the first mode period of the fixed-base structure. It should be noted that the soil condition and foundation are the same for both the MDOF super-structure and the equivalent SDOF oscillator. For the equivalent system only the MDOF super-structure is substituted with a SDOF oscillator.

The lateral stiffness and yielding strength are distributed over the structure height nonuniformly to account for higher-mode effects. To this end, the vertical distribution factor is computed as suggested by ASCE/SEI 7-10 standard. Thus, the story shear at any level (i^{th} story) can be

determined from the following equation:

$$V_i = C_{vi} V_b = (w_i h_i^k \Big/ \sum_{j=1}^{n} w_j h_j^k) V_b \tag{3}$$

C_{vi} and V_b stand for vertical distribution factor and base shear, respectively. w_i and w_j denote the portion of total effective weight of the structure assigned to the level i and j, in the same order. h_i and h_j represent the height from the structure base to the level i and j, correspondingly. k indicates an exponent related to the structure period taking value of 1 for structures with a period of 0.5 s or less, 2 for structures having a period of 2.5 s or more, and a linear interpolation is required for structures with periods between 0.5 and 2.5 s. Vertical distribution of the stiffness and yielding strength are based on the vertical distribution factor, C_{vi}. Accordingly, the stiffness and yielding strength at any level (i^{th} story) can be calculated using the following equations:

$$k_i = C_{vi} k_b \tag{4}$$

$$V_{yi} = C_{vi} V_{yb} \tag{5}$$

k_b is the stiffness associated with the base story which is computed so that the natural period of the fixed-base structure be same as the specified period. V_{yb} stands for the yielding strength corresponding to the base story that can be obtained from an iterative procedure in order to reach the specified structural ductility. Therefore, attempts are made to distribute the stiffness and strength along height of the structure based on the ASCE/SEI 7-10 standard so that it approximately complies with the stiffness and strength distribution in real structures.

The foundation is treated as a rigid body with no flexibility. m_0 and I_0 respectively stand for the mass and mass moment of inertia of the foundation. The foundation-to- super-structure mass ratio is selected between 0.2 and 0.5. A lumped-mass parameter model is adopted to represent the soil and the interaction mechanisms (Table 1).The soil beneath the foundation is considered as a homogenous half-space medium. Cone model was proposed by Meek and Wolf (1993) and Wolf (1994) for evaluating the dynamic stiffness of the soil. Comparing to the more rigorous numerical methods, the cone model requires only simple numerical manipulation within reasonable accuracy in engineering practices (Wolf 2004). The cone model substitutes the soil with a simplified 3-DOF system. The horizontal (sway), s, and the rocking, φ, degrees-of-freedom are introduced as the representatives of the translational and rotational motions of the foundation, respectively. u_s and φH_n indicate the horizontal displacement components caused by the sway and rocking motions at the roof story, respectively. u_n reflects the deformation that is associated with the strain in the super-structure. In order to take into account the frequency dependency of the soil, the additional internal rotational degree of freedom, θ, is assigned to a polar mass moment of inertia, m_θ, and connected to the foundation node using a rotational dashpot. In the case of nearly incompressible and incompressible soil (i.e., 0.33 < Poisson's ratio < 0.50), two features are included in to the soil model: (a) the axial-wave velocity, V_a, is restricted to two times the shear wave velocity, $2V_s$, (b) a trapped mass moment of inertia, ΔM_φ, of soil beneath the foundation, which moves as a rigid body in the same phase with the foundation for the rocking degree of freedom, is assigned to the foundation node. ΔM_φ is added to I_0 for the soil with Poisson's ratio greater than 0.3 (Wolf 2004). The coefficients of springs and dashpots for the sway and rocking motions are evaluated using the formulas presented in Table 1.

In Table 1, υ stands for the Poisson's ratio of soil which depends on the value of the shear wave

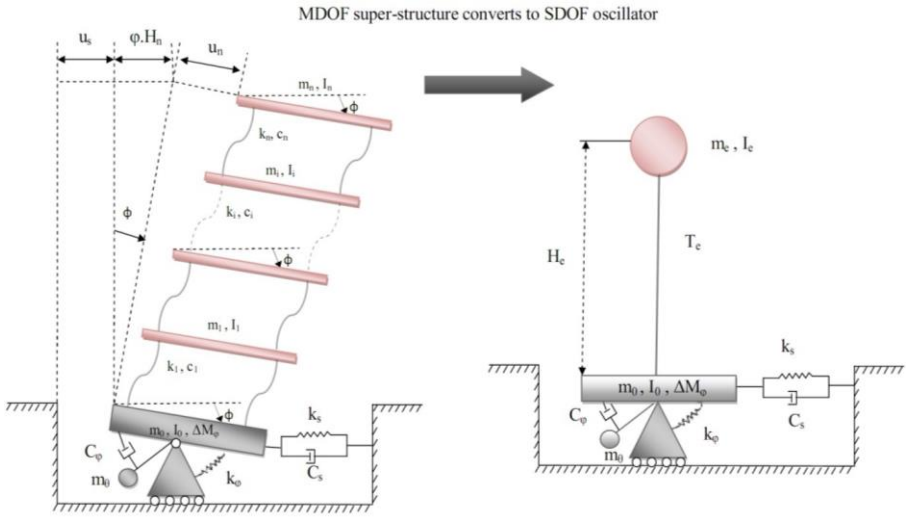

Fig. 1 Stick model of the MDOF super-structure and equivalent SDOF oscillator on the flexible soil medium

Table 1 Cone model for foundation on the surface of homogenous half-space soil

Lumped-Mass Parameter Model	
Rocking Motion	Sway Motion
$k_\varphi = 8\rho V_s^2 r^3/(3(1-\upsilon)$	$k_s = 8\rho V_s^2 r/(2-\upsilon)$
$C_\varphi = \pi\rho V_a r^4/4$	$C_s = \pi\rho V_s r^2$
$m_\theta = (9\pi^2/128)\rho r^5(1-\upsilon)(V_a/V_s)^2$	
$\Delta M_\varphi = 0.3\pi(\upsilon-0.33)\rho r^5$	

velocity. ρ represents the mass density of soil which depends on the shear wave velocity, too. A value of 2.35 t/m^3 is assigned to the mass density of soil for shear wave velocities higher than 750 m/s and for shear wave velocities lower than 750 m/s, a value of 1.95 t/m^3 is assumed. In order to model material damping of soil, non-linear-hysteretic damping is represented using frictional elements. Meek and Wolf (1994) demonstrated that the frequency- independent non-linear-hysteretic damping is more appropriate and may be realized by introducing frictional elements which permit causal analysis in the time domain. In this research, frictional elements are intended to analyze soil-structure problems and the soil material damping ratio is considered 5%.

Seismic behavior of soil–structure systems chiefly relies on the size, modal characteristics of the super-structure, and the soil attributes. It is demonstrated that the impacts of these factors can be taken into account by three parameters of non-dimensional frequency, aspect ratio and maximum story ductility (Ghannad *et al*. 1998). For the sake of incorporating soil flexibility condition into the studied systems, the non-dimensional frequency, a_0, is expressed as an indicator for the structure-to-soil stiffness ratio, $\omega_{fix}H_n/V_s$, where ω_{fix} is the circular frequency of the fixed-base structure. This indicator can have values up to 3 for customary buildings located on very soft

soils and values very close to zero are illustrative of fixed-base structures. In this study, this parameter is assumed 0, 1, 2, and 3 to cover the different intensities of soil flexibility. The aspect ratio of the super-structure which reflects the slenderness of the super-structure is defined as the ratio of total height of the super-structure to the foundation radius, i.e., H_n/r. In this paper, this parameter exercises various values of 1, 2, 3 and 4 to include a wide range of aspect ratios. These two factors are commonly selected as the key parameters of the soil-structure system (Ghannad *et al*. 1998). The n+3-DOF soil–structure model used in this research has the capability to be analyzed in the time domain. Herein, the model has been analyzed by using the βeta Newmark method. To accomplish this aim, a MATLAB (2011) code is developed to analyze the soil-structure systems. A deep sensitivity analysis is carried out employing the three key non-dimensional parameters μ, a_0 and H_n/r for structures with different heights. First, the yield base shear of the super-structure is calculated by iteration in order to reach the specified maximum story ductility in the assumed system within the accuracy of 1 % under the selected acceleration time history. Consequently, base shears of the MDOF and equivalent SODF super-structures are calculated for both fixed-base as well as flexible-base conditions.

3. Ground motion database

The ground motion database assembled for Nonlinear Time History (NTH) analyses of soil-structure system encompasses an extensive ensemble of near-fault ground motions. A total of 64 ground motions from fifteen earthquakes are chosen from Next Generation Attenuation (NGA) ground motion library (http://peer.berkeley.edu/nga). This ground motion ensemble is a subset of the records used by Baker (2007) and is related to soil type D and E. In Baker's study, the long-period directivity pulse and high-frequency components were quoted as Pulse and Residual, respectively. Fig. 2 illustrates Fourier Amplitude for original and decomposed components of E11 record (Table 2). As it is evident from Fig. 2, the original record contains a rich band of frequencies. It is decomposed to two components of pulse and high-frequency. The pulse component includes a simple and discernible pulse with the maximum Fourier Amplitude while

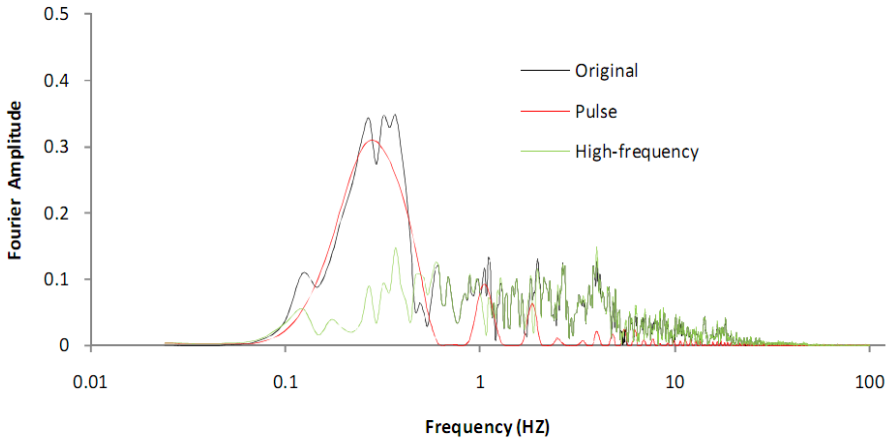

Fig. 2 Fourier transform for original and decomposed components of E11 record

Table 2 List of near-fault earthquake ground motions used in this study

Designation	Event	Year	Station	T_p	PGV (cm/s)	M_w	Epi. D.	Soil Type
E1	Imperial Valley-06	1979	Aeropuerto Mexicali	2.4	44.3	6.5	2.5	D
E2	Imperial Valley-06	1979	Agrarias	2.3	54.4	6.5	2.6	D
E3	Imperial Valley-06	1979	Brawley Airport	4.0	36.1	6.5	43.2	D
E4	Imperial Valley-06	1979	EC County Center FF	4.5	54.5	6.5	29.1	E
E5	Imperial Valley-06	1979	EC Meloland Overpass FF	3.3	115.0	6.5	19.4	D
E6	Imperial Valley-06	1979	El Centro Array #10	4.5	46.9	6.5	26.3	D
E7	Imperial Valley-06	1979	El Centro Array #11	7.4	41.1	6.5	29.4	D
E8	Imperial Valley-06	1979	El Centro Array #3	5.2	41.1	6.5	28.7	E
E9	Imperial Valley-06	1979	El Centro Array #4	4.6	77.9	6.5	27.1	D
E10	Imperial Valley-06	1979	El Centro Array #5	4.0	91.5	6.5	27.8	D
E11	Imperial Valley-06	1979	El Centro Array #6	3.8	111.9	6.5	27.5	D
E12	Imperial Valley-06	1979	El Centro Array #7	4.2	108.8	6.5	27.6	D
E13	Imperial Valley-06	1979	El Centro Array #8	5.4	48.6	6.5	28.1	D
E14	Imperial Valley-06	1979	El Centro Differential Array	5.9	59.6	6.5	27.2	D
E15	Imperial Valley-06	1979	Holtville Post Office	4.8	55.1	6.5	19.8	D
E16	Irpinia, Italy-01	1980	Sturno	3.1	41.5	6.9	30.4	D
E17	Westmorland	1981	Parachute Test Site	3.6	35.8	5.9	20.5	D
E18	Coalinga-07	1983	Coalinga-14th & Elm (Old CHP)	0.4	36.1	5.2	9.6	D
E19	Taiwan SMART1(40)	1986	SMART1 C00	1.6	31.2	6.3	68.2	D
E20	Taiwan SMART1(40)	1986	SMART1 M07	1.6	36.1	6.3	67.2	D
E21	N. Palm Springs	1986	North Palm Springs	1.4	73.6	6.1	10.6	D
E22	Whittier Narrows-01	1987	Downey - Co Maint Bldg	0.8	30.4	6.0	16.0	D
E23	Whittier Narrows-01	1987	LB - Orange Ave	1.0	32.9	6.0	20.7	D
E24	Superstition Hills-02	1987	Parachute Test Site	2.3	106.8	6.5	16.0	D
E25	Loma Prieta	1989	Alameda Naval Air Stn Hanger	2.0	32.2	6.9	90.8	E
E26	Loma Prieta	1989	Gilroy Array #2	1.7	45.7	6.9	29.8	D
E27	Loma Prieta	1989	Oakland - Outer Harbor Wharf	1.8	49.2	6.9	94.0	D
E28	Erzican, Turkey	1992	Erzincan	2.7	95.4	6.7	9.0	D
E29	Landers	1992	Barstow	8.9	30.4	7.3	94.8	D
E30	Landers	1992	Yermo Fire Station	7.5	53.2	7.3	86.0	D

Table 2 Continued

Designation	Event	Year	Station	T_p	PGV (cm/s)	M_w	Epi. D.	Soil Type
E31	Northridge-01	1994	LA - Wadsworth VA Hospital North	2.4	32.4	6.7	19.6	D
E32	Northridge-01	1994	Sylmar - Converter Sta	3.5	130.3	6.7	13.1	D
E33	Northridge-01	1994	Sylmar - Converter Sta East	3.5	116.6	6.7	13.6	D
E38	Chi-Chi, Taiwan	1999	CHY035	1.4	42.0	7.6	43.9	D
E39	Chi-Chi, Taiwan	1999	CHY101	4.8	85.4	7.6	32.0	D
E41	Chi-Chi, Taiwan	1999	TCU031	6.2	59.9	7.6	80.1	D
E42	Chi-Chi, Taiwan	1999	TCU036	5.4	62.4	7.6	67.8	D
E43	Chi-Chi, Taiwan	1999	TCU038	7.0	50.9	7.6	73.1	D
E44	Chi-Chi, Taiwan	1999	TCU040	6.3	53.0	7.6	69.0	E
E45	Chi-Chi, Taiwan	1999	TCU042	9.1	47.3	7.6	78.4	D
E46	Chi-Chi, Taiwan	1999	TCU049	11.8	44.8	7.6	38.9	D
E47	Chi-Chi, Taiwan	1999	TCU053	12.9	41.9	7.6	41.2	D
E48	Chi-Chi, Taiwan	1999	TCU054	10.5	60.9	7.6	37.6	D
E49	Chi-Chi, Taiwan	1999	TCU056	12.9	43.5	7.6	39.7	D
E50	Chi-Chi, Taiwan	1999	TCU060	12.0	33.7	7.6	45.4	D
E51	Chi-Chi, Taiwan	1999	TCU065	5.7	127.7	7.6	26.7	D
E52	Chi-Chi, Taiwan	1999	TCU068	12.2	191.1	7.6	47.9	D
E53	Chi-Chi, Taiwan	1999	TCU075	5.1	88.4	7.6	20.7	D
E54	Chi-Chi, Taiwan	1999	TCU076	4.0	63.7	7.6	16.0	D
E55	Chi-Chi, Taiwan	1999	TCU082	9.2	56.1	7.6	36.2	D
E56	Chi-Chi, Taiwan	1999	TCU098	7.5	32.7	7.6	99.7	D
E57	Chi-Chi, Taiwan	1999	TCU101	10.0	68.4	7.6	45.1	D
E58	Chi-Chi, Taiwan	1999	TCU102	9.7	106.6	7.6	45.6	D
E59	Chi-Chi, Taiwan	1999	TCU103	8.3	62.2	7.6	52.4	D
E60	Northwest China-03	1997	Jiashi	1.3	37.0	6.1	19.1	D
E61	Yountville	2000	Napa Fire Station #3	0.7	43.0	5.0	9.9	D
E62	Chi-Chi, Taiwan-03	1999	CHY024	3.2	33.1	6.2	25.5	D
E63	Chi-Chi, Taiwan-03	1999	TCU076	0.9	59.4	6.2	20.8	D
E64	Chi-Chi, Taiwan-06	1999	CHY101	2.8	36.3	6.3	50.0	D

the high-frequency part contains a band of frequencies with smaller values of Fourier Amplitudes.

A complete list of the original records and their corresponding features such as the pulse period (T_p), the Peak Ground Velocity (PGV), and the Epicentral Distance (Epi. D.) are presented in Table 2.

Baker developed a procedure to extract the largest velocity pulse from a record. The procedure consists of using the wavelet transform to identify the dominant pulse of the record. Baker used the size of the extracted pulse relative to the original ground motion to develop a quantitative criterion to classify a ground motion as pulse-like. To identify the pulse-like records potentially caused by directivity effects, two additional criteria were applied: the pulse arrives at the beginning of the strong ground motion and the absolute amplitude of the velocity pulse is large relative to the remainder of the record.

4. Evaluation of higher-mode effects for the assumed soil-MDOF structure systems

In this section, it is intended to measure the severity of higher-mode effects for the soil-structure systems subjected to the pulse and high-frequency components of near-fault ground motions. To evaluate the higher-mode effects, base shear is chosen as a primary engineering demand parameter. Base shear is a desirable demand for force-based design procedures which is included in the seismic codes. Therefore, the MDOF systems and their respective equivalent SDOF systems described in the section 2 are analyzed under the two prominent components of 64 near-fault ground motions presented in section 3 and the peak of base shears determined from NTH analysis is obtained. It is more tangible if the higher-mode effects can be quantified in the term of a parameter. In this regard, α_M parameter is defined as the following:

$$\alpha_M = \frac{V_{MDOF}^{\mu}}{V_{SDOF}^{\mu}} \tag{6}$$

V_{MDOF}^{μ} and V_{SDOF}^{μ} correspond to the base shear of MDOF and equivalent SDOF super-structures at the specific maximum story ductility of μ, respectively. The subscript of M is accounted for higher-modes. This parameter can be used as a modification factor to convert the results of a SDOF system to the corresponding MDOF one. In the following, for all graphs, the horizontal axis shows the pulse period extracted by wavelet analysis (Baker 2007). In the previous studies like Iervolino *et al*. (2010), it has been confirmed that the pulse period (T_p) is expected to be the most important feature of this kind of ground motions. Additionally, it should be noted that for the sake of brevity all graphs are skipped to be presented for all values of non-dimensional frequencies and aspect ratios. Herein, to draw main conclusions, only values corresponding to extreme conditions, i.e., values of 0 (fixed-base structures) and 3 (dominant SSI effects) for the non-dimensional frequency and values of 1 (squatty structures) and 4 (slender structures) for the aspect ratio are represented. However, the results hold for other values of the non-dimensional frequency and aspect ratio not shown here.

Fig. 3 illustrates the variation of α_M parameter of the fixed-base structure (a_0=0) for both pulse and high-frequency components with increasing the pulse period. The red plot represents the α_M parameter for the pulse component while the green one shows the α_M parameter for the high-frequency component. For the pulse record, as Fig. 3 represents, the plots have a relatively regular trend. The value of α_M parameter decreases as the pulse period increases. It should be noted that

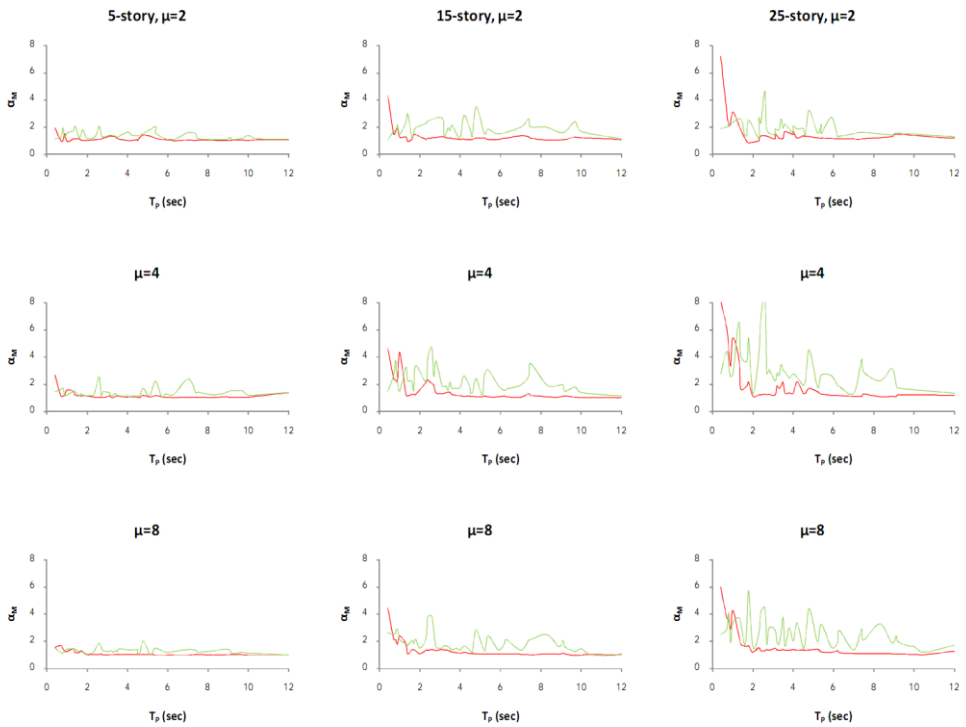

Fig. 3 values of αM parameter for the fixed-base structures with different number of stories

the pulse record has simple frequency-content and contains only a distinctive directivity pulse.

For very short-period pulses, the pulse component has larger values of α_M parameter and it implies that the higher-mode effects are more significant for very short-period pulses than long-period pulses.It can be explained by the proximity of short-period pulses to the periods pertained to the higher modes of the structure. In such situation, the higher modes are activated strongly and the structural responses are more dependent on the higher modes such that the value of α_M parameter reaches more than 1. For the 25-story structure, the value of α_M parameter corresponds to nearly 8. However, as the pulse period elongates, they become very far from higher mode periods of the structure and the first mode is the dominant mode. Therefore, the value of α_M parameter complies nearly with 1. It means that the base shear of the structure can be obtained from its equivalent SDOF oscillator with an acceptable accuracy.

Increasing the maximum story ductility from 2 to 4 amplifies the value of α_M parameter for very short-period pluses. However, the value of α_M parameter still remains nearly 1 for long-period pulses. As the maximum story ductility increases, the effective period of the structure elongates and higher mode periods comply more significantly with the pulse periods. This also causes the boundary pulse period between short and long period pulses to elongate and plots pertaining to pulse records shift to the right. On the contrary, further scrutiny for higher maximum story ductility, i.e., 8, reveals that the value of α_M parameter mitigates in comparison with maximum story ductility of 4. In this case, effective period of the structure elongates such that it becomes

very far from some periods of the structure and the severity of higher-mode effects decreases. Number of stories also has consequential effects on the higher modes excitation. As it is evident from Fig. 3, increasing the number of stories magnifies the intensity of higher-mode effects, particularly for very short-period pulses. It is obvious that increasing the story number provides the structure with much more number of higher modes and this makes the situation easier for triggering higher modes.

On the other side, the plots related to the high-frequency record have erratic trends. In some pulse periods, it possesses a distinguishable peak for α_M parameter while in some cases, it approaches to 1. To explain this phenomenon, it should be noted that high-frequency record, in spite of the pulse record, encompasses a band of frequencies which is very rich in frequency-content. Therefore, the value of α_M parameter depending upon which mode or modes are activated by such frequencies can have a notable peak or a small value very close to 1. Thus, an irregular pattern for α_M parameter is obtained. For the high-frequency record, the effects of story number and maximum story ductility are the same as the pulse record. As the number of stories increases, a better situation is provided for high frequencies to activate higher modes. Also, maximum story ductility makes the effective period of the structure to elongate and for low story ductility, i.e., 2 and 4, the high-mode effects become more severe. However, for the high story ductility, i.e., 8, the intensity of higher-mode effects mitigates due to the large difference between high frequencies of the record and the effective frequencies of the structure. Comparing values of α_M parameter for the pulse and high-frequency records discloses that for very short-period pulses, the contribution of the pulse part to the higher-mode effects is more significant than the high-frequency one. This implies that near-fault ground motions with very short-period pulses, up to about 1 sec, are not very diverse in frequency-content due to the short duration of the record and the pulse component is the dominant frequency for activation of higher modes. For other pulse periods, the high frequency part is more pronounced and is more capable to trigger higher modes of the structures. For the high-frequency portion, the value of α_M parameter is much more than 1 in most cases while for pulse portion, the value of α_M parameter oscillates about one. It indirectly implies that for the high-frequency part, the demands of the structure cannot be computed based on its corresponding equivalent SDOF oscillator. This note should be emphasized that increasing the story number amplifies the phenomenon. Also, the maximum story ductility, as mentioned previously, has increasing and mitigating effects for lower and higher maximum story ductility, respectively.

From earlier discussion, this indirectly revealed that ignoring the high-frequency component of near-fault ground motions and cutting them off from the original record will lead to the responses which cannot be reliable. As it was mentioned, high-frequency records cause the higher-modes to activate more significantly than pulse record and this might result in the higher responses for structures. As previously discussed, the effects of soil flexibility can be best described by the non-dimensional frequency parameter. This parameter emphasizes that the severity of soil-structure interaction primarily depends on the ratio of structure-to-soil stiffness not soil alone. In this case, as the non-dimensional frequency increases, the interaction between the soil and the structure becomes more meaningful. For conventional structures, the peak value for non-dimensional frequency is assumed 3.

The interaction mechanism can affect the structural responses via two important sources. First, the stiffness reduction of the overall system that leads to the period elongation of the system. Second, the radiation damping of the system that emanates from the propagation of structural energy through the semi-infinite medium of soil. Fig. 4 illustrates the effects of soil flexibility

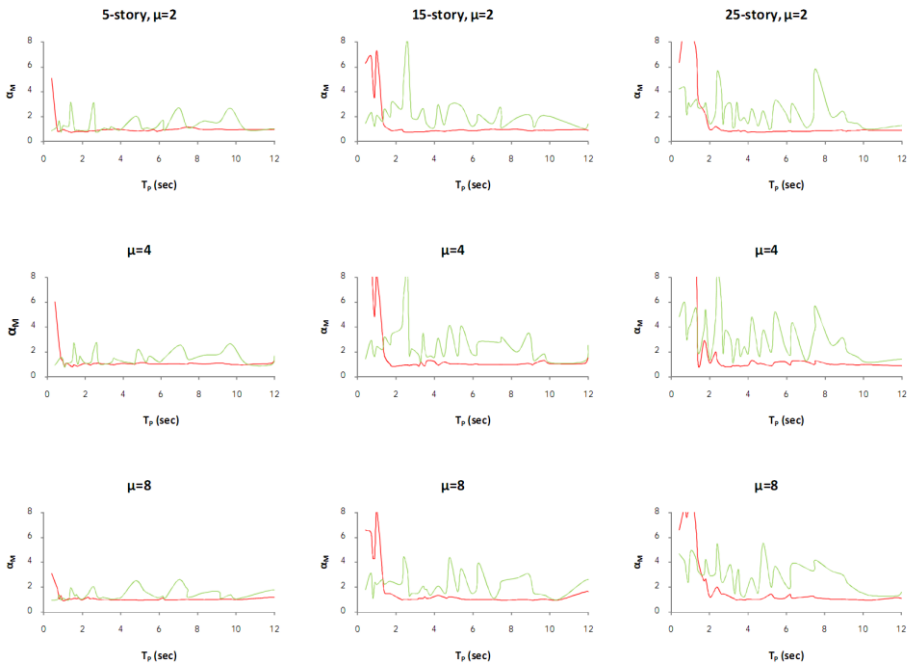

Fig. 4 values of αM parameter for the soil-structure system (a_0=3, Hn/r=4) with different number of stories

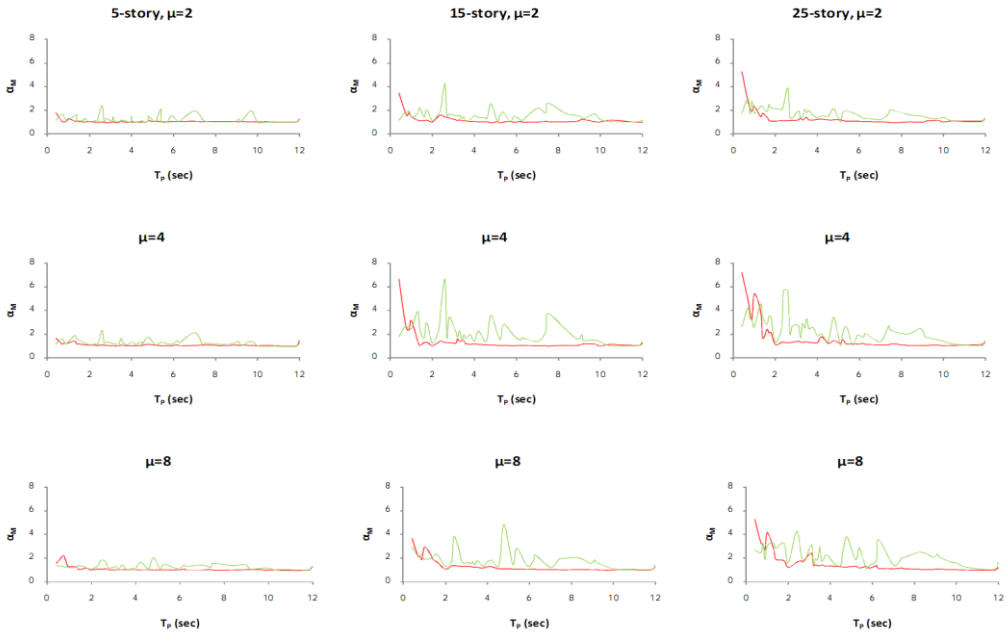

Fig. 5 values of α_M parameter for the soil-structure system (a_0=3, H_n/r=1) with different number of stories

on the value of α_M parameter for non-dimensional frequency of 3 and aspect ratio of 4. As it is obvious from Fig. 4, for pulse records, the values of α_M parameter are amplified by SSI effects for short-period pulses. It indicates that the higher-mode effects are more sever with the presence of soil beneath the structure. The vibration Period of the soil-structure system is longer than the fixed-base one. This period elongation causes the period of higher modes to increase and comply with the pulse period.

However, for long-period pulses, the values of α_M parameter approaches to 1 and the SSI effects do not affect the α_M parameter in this pulse-period range. Although it is well-known that SSI effects significantly affect the seismic response of the structure and radiation damping leads to reduce the base shear for both the MDOF and equivalent SDOF super-structures, it should be noted that the ratio of both base shears is an indicator for high-mode effects not each one of them alone. The mitigation of base shear does not imply that higher-mode effects must be reduced since overall stiffness reduction of the system renders higher modes to be more responsive to pulse periods.

Also, the effects of the number of stories and maximum story ductility are the same as the fixed-base condition. For high-frequency records, SSI effects also have amplifying consequences and make the higher modes contribute more to the response of the system. The variation of α_M parameter has not a definite order and the irregularity of plots is due to the complicated frequency-content of the high-frequency portion of the original records. Comparing pulse and high-frequency parts gives some important notes.

For very-short period pulses, the capability of the pulse part of the original record to activate higher modes of the structure is much more than the high-frequency part. For longer pulse periods, the variation is vice-versa and higher-mode effects are more significant for the high-frequency portion. Also, the previously mentioned boundary pulse period is moved toward right due to the SSI effects. The reason lies in the period elongation of the system due to the soil flexibility.

Another important key parameter which considerably affects the response of soil-structure systems is the aspect ratio. Fig. 5 illustrates the values of α_M parameter for non-dimensional frequency of 3 and aspect ratio of 1. Comparing Fig. 4 and 5 gives an insight to the effects of the aspect ratio on higher modes. For soil-structure systems, as the aspect ratio decreases or the super-structure becomes squatty, the period of the system shortens. Furthermore, the increasing rate of radiation damping grows for squatty structures compared to slender ones. For pulse record, the value of α_M parameter mitigates due to the reduction of the aspect ratio particularly for very short-period pulses. For high-frequency record, the values of α_M parameter reduce for squatty structures in comparison with slender structures. This implies that the severity of higher-mode effects lessens for squatty structures. Comparison of α_M values related to pulse and high-frequency parts discloses that the two plots become tight together and their difference becomes smaller. The reason lies in the rapid increasing rate of radiation damping which mitigates the input energy of the records.

However, at very-short periods, the effects of pulse records on α_M parameter are more significant and as the pulse period increases, the high-frequency part becomes dominant. Moreover, the boundary pulse period shifts toward left compared to slender structures because of period shortening of the system due to the reduction of aspect ratio.

5. Conclusions

In this study, attempts are made to carry out a deep parametric investigation on estimation of higher-mode effects for nonlinear soil-structure systems under different components of near-fault ground motions. To this end, the super-structure and soil are simulated on the basis of Stick model and Cone model, respectively. Pulse and high-frequency parts of 64 near-fault ground motions are intended to use for NTH analyses. The ratio of base shear related to soil-MDOF structure system to its corresponding equivalent soil-SDOF system, α_M parameter, is used to estimate the severity of higher-mode effects.

The results verify that the value of α_M parameter for pulse record has a regular trend with respect to pulse period due to the simple frequency-content of the record and for very short-period pulses, its corresponding α_M value is significant and as the pulse period increases, it reaches to 1. For high-frequency record, an erratic pattern is achieved owing to the complicated frequency-content of high-frequency part. Higher-mode effects for very short-period pulses is very notable for pulse record in comparison with the high-frequency one. However, for longer period pulses, it is the high-frequency part that is governing and has more consequences on the severity of higher-mode effects. Also, a boundary period is observed above which high-frequency effects is predominant.

SSI effects result in the higher values of α_M parameter compared to fixed-base condition for very short period of pulse record. Also, the effects of high-frequency record on higher modes become consequential under SSI effects. The boundary pulse period shifts toward right due to the period elongation of the system. Moreover, as the structure becomes squatty the higher-mode effects mitigates and the boundary pulse period moves toward left due to the period shortening of the system. For low maximum story ductility, nonlinearity effect has an increasing impact on higher -mode effects; however, for high story ductility, the phenomenon is reversed. Moreover, increasing number of stories provides a better situation for higher modes and such effects become meaningful.

References

Alavi, B. and Krawinkler, H. (2004), "Behaviour of moment resisting frame structures subjected to near-fault ground motions", *Earthq. Eng. Struct. Dyn.*, **33**, 687-706.

ASCE/SEI 7-10 9 (2010), "Minimum Design Loads for Buildings and Other Structures", Published by American Society of Civil Engineers.

Aviles, J. and Perez-Rocha, L.E. (2003), "Soil–structure interaction in yielding systems", *Earthq. Eng. Struct. Dyn.*, **32**, 1749-1771.

Aviles, J. and Perez-Rocha, L.E. (2005), "Influence of Foundation Flexibility on R_μ and C_μ Factors", *J. Struct. Eng., ASCE*, **131**(2), 221-230.

Aviles, J. and Perez-Rocha, L.E. (2011), "'Use of global ductility for design of structure-foundation systems", *Soil Dyn. Earthq. Eng.*, **31**, 1018-1026.

Baker, J.W. (2007), "Quantitative classification of near-fault ground motions using wavelet analysis", *Bull. Seismol. Soc. Am.*, **97**(5), 1486-1501.

Bielak, J. (1978), "Dynamic response of non-linear building-foundation systems", *Earthq. Eng. Struct. Dyn.*, **7**, 17-30.

Chopra, A.K. and Gutierrez, J.A. (1974), "Earthquake response analysis of multistory building including foundation interaction", *Earthq. Eng. Struct. Dyn.*, 2002, 65-77.

Elsheikh, A. and Ghobarah, A. (2004), "Response of RC structures to near-fault records", *Emirates J. Eng. Res.*, **9**(2), 45-51.
FEMA 440 (2005), "Improvement of nonlinear static seismic analysis procedures", Federal Emergency Management Agency, Washington DC, US.
Ghahari, S.F., Jahankhah, H. and Ghannad, M.A. (2010), "Study on elastic response of structures to near-fault ground motions through record decomposition", *Soil Dyn. Earthq. Eng.*, **30**, 536-546.
Ghannad, M.A., Fukuwa, N. and Nishizaka, R. (1998), "A study on the frequency and damping of soil–structure systems using a simplified model", *J. Struct. Eng., ASCE*, **44**, 85-93.
Ghannad, M.A. and Ahmadnia, A. (2006), "The effect of soil–structure interaction on the inelastic structural demands", *Euro. Earthq. Eng.*, **20**(1), 23-35.
Ghobarah, A. (2004), "Response of structures to near-fault ground motion", *Proceedings of the 13th World Conference on Earthquake Engineering*, Vancouver, B.C., Canada.
Hubbard, D.T. and Mavroeidis, G.P. (2011), "Damping coefficients for near-fault ground motion response spectra", *Soil Dyn. Earthq. Eng.*, **31**, 401-417.
Iervolino, I., Chioccarelli, E. and Baltzopoulos, G. (2012), "Inelastic displacement ratio of near-source pulse-like ground motions", *Earthq. Eng. Struct. Dyn.*, DOI: 10.1002/eqe.2167.
Kalkan, E. and Kunnath, S.K. (2006), "Effects of fling step and forward directivity on seismic response of buildings", *Earthq. Spect.*, **22**(2), 367-390.
Kam, W.Y., Pampanin, S., Palermo, A. and Carr, A.J. (2010), "Self-centering structural systems with combination of hysteretic and viscous energy dissipations", *Earthq. Eng. Struct. Dyn.*, **39**(10), 1083-1108.
Mavroeidis, G.P. and Papageorgiou, A.S. (2002), "Near-source strong ground motion: characteristics and design issues", *Proceedings of the Seventh U.S. National Conference on Earthquake Engineering (7NCEE)*, Boston, Massachusetts.
Mavroeidis, G.P. and Papageorgiou, A.S. (2003), "A mathematical representation of near- fault ground motions", *Bull. Seismol. Soc. Am.*, **93**(3), 1099-1131.
Mavroeidis, G.P., Dong, G. and Papageorgiou, A.S. (2004), "Near-fault ground motions, and the response of elastic and inelastic single-degree-freedom (SDOF) systems", *Earthq. Eng. Struct. Dyn.*, **33**, 1023-1049.
Mylonakis, G. and Reinhorn, A.M. (2001), "Yielding oscillator under triangular ground acceleration pulse", *J. Earthq. Eng.*, **5**, 225-251.
Mylonakis, G. and Voyagaki, E. (2006), "Yielding oscillator subjected to simple pulse waveforms: numerical analysis&closed-form solutions", *Earthq. Eng. Struct. Dyn.*, **35**(15), 1949-1974.
Nakhaei, M. and Ghannad, M.A. (2004), "Effect of soil–structure interaction on energy dissipation of buildings", *Proceedings of ICEBAM international conference on earthquake engineering*, A Memorial of Bam Disaster, Paper Reference 1066.
Nakhaei, M. and Ghannad, M.A. (2008), "The effect of soil–structure interaction on damage index of buildings", *Eng. Struct.*, **30**, 1491-1499.
Novak, M. (1974), "Effect of soil on structural response to wind and earthquake", *Earthq. Eng. Struct. Dyn.*, **3**, 79-96.
Makris, N. and Roussos, Y. (1998), *Rocking Response and Overturning of Equipment under Horizontal Pulse-Type Motion*, Pacific Earthquake Engineering Research Center (PEER), Report No. 05.
MATLAB software, version 2011, MATtrix LABoratory, http://www.mathworks.com.
Meek, W. and Wolf, J.P. (1993), "Why cone models can represent the elastic half-space", *Earthq. Eng. Struct. Dyn.*, **22**, 759-771.
Meek, W. and Wolf, J.P. (1994), "Material Damping for Lumped-Parameter Models of Foundation", *Earthq. Eng. Struct. Dyn.*, **23**, 349-362.
Muller, F.P. and Keintzel, E. (1982), "Ductility requirements for flexibly supported antiseismic structures", *Proceedings of the 7th European conference on earthquake engineering*.
Rodriguez, M.E. and Montes, R. (2000), "Seismic response and damage analysis of buildings supported on flexible soils", *Earthq. Eng. Struct. Dyn.*, **29**, 647-665.
Seekings, L.C. and Boatwright, J. (2010), "Rupture directivity of moderate earthquakes in Northern

California", *Bull. Seimol. Soc. Am.*, **100**(3), 1107-1109.
Sehhati, R., Rodriguez-Marek, A., ElGawady, M. and Cofer, W.F. (2011), "Effects of near-fault ground motions and equivalent pulses on multi-story structures", *Eng. Struct.*, **33**, 767-779.
Shiming, W. and Gang, G. (1998). Dynamic soil-structure interaction for high-rise buildings, *Developments Geotech. Eng.*, **83**, 203-216.
Spudich, P. and Chiou, B.S.J. (2008), "Directivity in NGA earthquake ground motions: analysis using isochrone theory", *Earthq. Spect.*, **24**(1), 279-298.
Somerville, P.G., Smith, N.F., Graves, R.W. and Abrahamson, N.A. (1997), "Modification of empirical strong motion attenuation relations to include the amplitude and duration effects of rupture directivity", *Seismol. Res. Lett.*, **68**(1), 199-222.
Somerville, P.G. (2000), "New developments in seismic hazard estimation", *Proceedings of the Sixth International Conference on Seismic Zonation*, Palm Springs, California.
Takewaki, I. (1998), "Equivalent linear ductility design of soil-structure interaction systems", *Eng. Struct.*, **20**(8), 655-662.
Tang,Y. and Zhang, J. (2011), "Response spectrum-oriented pulse identification and magnitude scaling of forward directivity pulses in near-fault ground motions", *Soil Dyn. Earthq. Eng.*, **31**, 59-76.
Veletsos, A.S. (1977), "Dynamic of structure-foundation systems", In: Hal WJ, Ed. Structural and Geotechnical Mechanics, Englewood Cliffs (NJ): Prentice-Hall.
Wolf, J.P. (1994), "Foundation vibration analysis using simple physical models", Englewood Cliffs (NJ): Prentice-Hall.
Wolf, J.P. and Deeks, A.J. (2004), "Foundation vibration analysis: a strength-of-materials approach".
Xu, Z. and Agrawal, A. (2010), "Decomposition and effects of pulse components in near-field ground Motions", *J. Struct. Eng.*, **136**(6), 690-699.
Zhang, Y. and Iwan, W.D. (2002), "Active interaction control of tall buildings subjected to near-field ground motions", *J. Struct. Eng.*, **128**, 69-79.